Suitability of swelling and collapse theory proposed based on virgin compression surface

HOSTED BY

ELSEVIER

Available online at www.sciencedirect.com

ScienceDirect

Soils and Foundations xxx (xxxx) xxx

SOILS AND FOUNDATIONS

www.elsevier.com/locate/sandf

Technical Paper

Suitability of swelling and collapse theory proposed based on virgin compression surface

Asmaa Al-Taie [a], Mahdi Disfani [a,*], Ehsan Yaghoubi [b]

[a] Department of Infrastructure Engineering, The University of Melbourne, Melbourne, Australia
[b] College of Engineering and Science, Victoria University, Melbourne, Australia

Received 26 November 2019; received in revised form 26 October 2020; accepted 18 November 2020

Abstract

This study investigates the suitability of the swelling and collapse theory proposed based on a constitutive virgin compression surface (VCS) developed within the modified Monash Peradeniya Kodikara (MPK) framework. The modified MPK approach incorporates net stress, void ratio, and moisture ratio as state variables to interpret the swelling-collapse behavior of unsaturated soils. The soil selected for this research was an expansive Quaternary age basaltic residual clay located in Victoria, Australia. The experimental program included testing on unsaturated compacted clay specimens and clay specimens stabilized with lime at the optimum lime content (OLC). The OLC was obtained based on the swelling potential. Static compaction tests were conducted on untreated and lime-treated samples to establish the VCS and to propose the relationship between moisture ratio and net stress. Next, 1-D compression and consolidation laboratory tests were carried out to investigate and compare the mechanism of collapse and swelling based on well-established suction-based theories and the moisture content-based approach of this research. The swelling and collapse response obtained through both theories were very close which verified the suitability of the moisture content-based approach, being the Modified MPK framework. This study also investigated the application of suction-controlled experimental data extracted from the relevant literature within the modified MPK framework. The novelty of this study is proposing and validating a framework for conversion of the results between two different partial theories to interpret the volumetric behavior of expansive clay. Finally, a new method is proposed to estimate the swelling-collapse state of a sample through wetting without the need to establish the VCS.

Keywords: Collapse and swelling; Expansive clays; Lime treatment; Modified MPK framework; Soil suction

1. Introduction

Most available constitutive models use net stress and suction as constitutive parameters to describe the volumetric behavior of unsaturated soils (Alonso et al., 1990; Fredlund and Morgenstern, 1976; Ghasemzadeh et al., 2017; Loret and Khalili, 2002; Rahardjo et al., 2018; Sheng et al., 2008; Sivakumar and Wheeler, 2000; Takayama et al., 2017; Wheeler and Sivakumar, 1995). Alonso et al. (1990), Wheeler and Sivakumar (1995), and Sivakumar and Wheeler (2000) presented constitutive models for illustrating the stress-strain relationship of unsaturated soils. The Barcelona Basic Model (BBM) (Alonso et al., 1990), used two independent stress variables, being net mean stress and suction. The BBM framework formulated a model for isotropic stress states, including yield stress. A proper stress space was used to describe the isotropic states (σ, s), where net mean stress (σ) is the excess

Peer review under responsibility of The Japanese Geotechnical Society.
* Corresponding author at: Melbourne School of Engineering, The University of Melbourne, Parkville, VIC 3010, Australia.
E-mail addresses: aaltaie@unimelb.edu.au (A. Al-Taie), mahdi.miri@unimelb.edu.au (M. Disfani), ehsan.yaghoubi@vu.edu.au (E. Yaghoubi).

https://doi.org/10.1016/j.sandf.2020.11.003
0038-0806/

Please cite this article as: A. Al-Taie, M. Disfani and E. Yaghoubi, Suitability of swelling and collapse theory proposed based on virgin compression surface, Soils and Foundations, https://doi.org/10.1016/j.sandf.2020.11.003

of mean stress over air pressure and s is the suction. The BBM can be considered as the first elasto-plastic model that is mostly used to describe the volumetric behavior of unsaturated soils. However, other behaviors of partially saturated soils, such as changes in moisture content or the degree of saturation have not been covered in the BBM model.

Kodikara (2012) proposed a new framework, called Monash-Peradeniya-Kodikara (MPK), to describe the volumetric behavior of compacted unsaturated soils. This model incorporates void ratio (e), net stress (σ) and moisture ratio (e_w) (i.e. the product of the specific gravity and moisture content) as state variables. The MPK framework has been verified through research works presented in several publications such as Kodikara et al. (2016) and Islam and Kodikara (2016). This framework has also been extended to unsaturated granular material applications by Yaghoubi et al. (2019) and extended to shear behavior by Abeyrathne (2017). An important feature of the MPK framework is linking the constitutive deformation behavior of soils and the traditional compaction curves. In principle, any variable with the potential for a considerable effect on mechanical behavior can be taken as a state variable (Lu, 2008). Therefore, both moisture content and suction could be considered a state variable, as the volume change of soils could be affected by these variables (Fredlund and Rahardjo, 1993). The Monash-Peradeniya-Kodikara framework points out that moisture content is a practical method in interpreting the deformation caused by swell-shrink cycles and the deformation of soils under a loading-unloading path, and wetting under constant net stress (Kodikara et al., 2014). The use of moisture ratio does not undermine the work that can be achieved on hysteresis with suction. It is important to develop an approach where some difficulties associated with unsaturated testing and analysis can be avoided. Kodikara adopted the compaction curves to create the virgin compression surface as shown in Fig. 1. Based on the MPK framework, the variation of e_w with respect to e could be described as a function of cosine presented in Eq. (1).

$$\frac{e}{e_s} = \left[\left(\frac{e_0}{e_s} - 1\right)\cos\left(\frac{\varphi e_w}{e_s}\right) + \left(1 - \frac{e_0}{e_s}\cos(\varphi)\right)\right]\frac{1}{1-\cos(\varphi)} \tag{1}$$

$$e_s = e_{s0} - \lambda_{sat}\ln\sigma \tag{2}$$

$$e_0 = e_0^* - \lambda_{dry}\ln\sigma \tag{3}$$

where $\varphi = \pi/(e_{wc}/e_s)$ and e_{wc} is the optimum moisture ratio for net stress σ, e_0 is the void ratio at $e_w = 0$ (degree of saturation, $S_r = 0$) for net stress σ and e_s is the void ratio on Normally Consolidated Line, NCL ($S_r = 1$) for stress σ. The compaction curve corresponding to $\sigma = 1$ kPa shows the loosest state where e_0^* and e_{s0} represent the void ratios at $e_w = 0$ and on saturation line (on NCL), respectively. λ_{dry} and λ_{sat} are the gradient of the compression line at dry and saturated states. Based on Eqs. (1)–(3) the cosine function begins from $e_w = 0$ ($S_r = 0$) (Kodikara, 2012).

However, Al-Taie et al. (2019) suggested that the function of cosine begins from a particular degree of saturation described as S_r^* as shown in Fig. 2. Thus, the surface is divided into two parts, being **A** and **B**, by S_r^* line as shown in Fig. 2. Part **A** represents the surface where the original MPK model is valid, and part **B** represents the surface where the original MPK is not valid. Part **A** applies to specimens prepared at a degree of saturation higher than S_r^* or compacted under higher net stresses applied in this research project (≥1000 kPa for the untreated expansive clay and ≥500 kPa for stabilized clay which are both corresponding

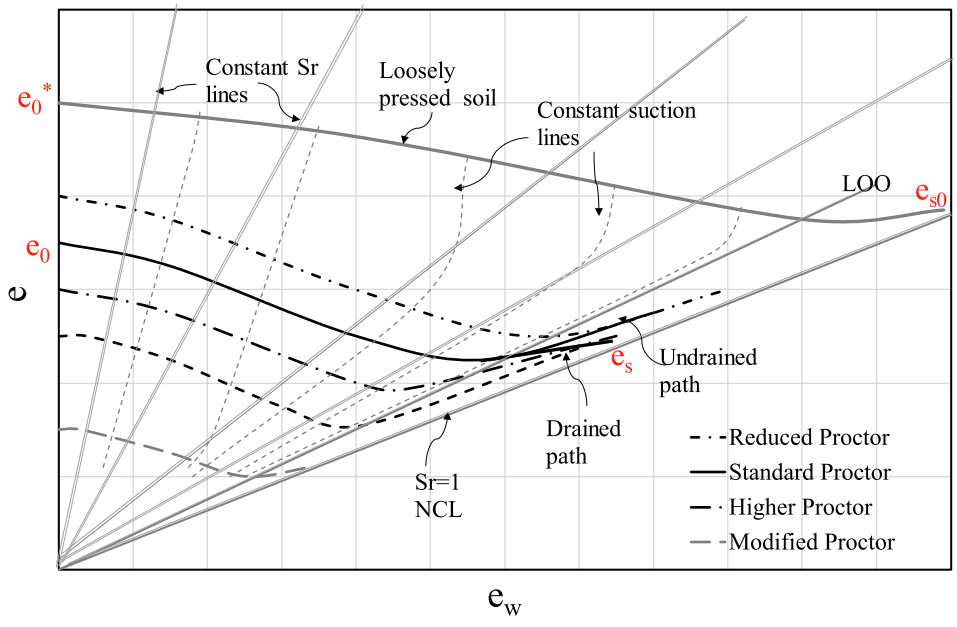

Fig. 1. Virgin compaction surface proposed by Kodikara (2012).

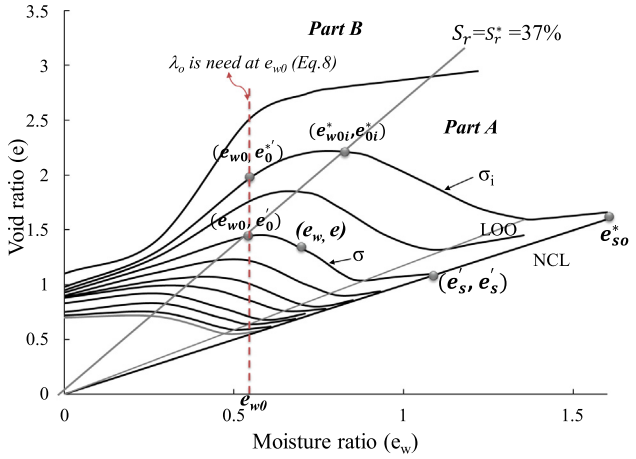

Fig. 2. Modified MPK framework.

to about $e \leq 0.75$). Kodikara (2012) suggested that the compaction curve corresponding to $\sigma = 1$ kPa represented the loosest state. Such low stress may not be adequate to form a compaction curve, especially when a sample is prepared at a high degree of saturation. Therefore, it is suggested to choose another compaction curve at $\sigma = \sigma_i$ where the cosine function is clearly seen. This curve can be considered as the loosest state, where e_{0i}^* and e_{so}^* represent the void ratios at $e_w = e_{w0i}^*$ (at S_r^*) and on NCL, respectively. Consequently, the original MPK framework (Eq. (1)) was modified to take into account the degree of saturation of S_r^* and the loosest state. Accordingly, the modified MPK model was developed by Al-Taie et al. (2019) and is expressed as follows:

$$\frac{e}{e_s'} = \left[\left(\frac{e_0'}{e_s'} - 1\right)\cos\left(\frac{\varphi(e_w - e_{w0})}{e_s' - e_{w0}}\right) + \left(1 - \frac{e_0'}{e_s'}\cos(\varphi)\right)\right]\frac{1}{1-\cos(\varphi)} \tag{4}$$

$$e_0' = \frac{e_{w0}}{S_r^*} \tag{5}$$

$$\sigma = \left(e^{\left(e_0^{*'} - e_0'\right)/\lambda_0}\right) \times \sigma_i \tag{6}$$

$$e_s' = e_{so}^* - \lambda_{sat}\ln\left(\frac{\sigma}{\sigma_i}\right) \tag{7}$$

$$\lambda_0 = ae_w + b \tag{8}$$

where e_{w0} is the initial moisture ratio where the cosine function of the compaction curve starts at the stress of σ and degree of saturation of S_r^*, e_0' is the initial void ratio where the cosine function of the compaction curve starts at the stress of σ, moisture ratio of e_{w0} and degree of saturation of S_r^*, e_{w0i}^* is the initial moisture ratio where the cosine function of the compaction curve starts at $\sigma = \sigma_i$ and degree of saturation of S_r^*, the e_{w0i}^* does not appear in Eqs. (4)–(8) as this parameter is just an indicator for values of e_{w0}. It is obvious from Fig. 2 that the stress level increases as the e_{w0} decreases (the curves shift towards the left as the stress increases). As all compaction curves are established at a stress level higher than the loosest curve ($\sigma = \sigma_i$), all e_{w0} are expected to be less than e_{w0i}^*. $e_0^{*'}$ is the void ratio at $\sigma = \sigma_i$, and the moisture ratio of e_{w0} ($e_{w0} < e_{w0i}^*$), λ_0 is the gradient of compression line at $e_w = e_{w0}$ (Eq. (8)), e_s' is the void ratio at saturation (on NCL) and stress σ, e_{so}^* is the void ratio at saturation and stress σ_i, a and b are fitting parameters. For the untreated clay specimens, the values of a and b are 0.4494 and 0.0609, respectively; and, for the treated clay specimens, the values of a and b are 0.174 and 0.1027, respectively (Al-Taie et al., 2019).

Al-Taie et al. (2019) proposed a method to predict the swelling and collapse potential after wetting. A constant void ratio line (LV) can be plotted on the surface by identifying the moisture ratio, compaction stress and corresponding void ratio. If specimens were wetted under a stress located at the LV, specimens collapsed and the value of collapse could be predicted. However, if specimens were wetted under a stress above the LV, the specimens swelled and the value of swelling would depend on the gradient of swelling.

The current study looks at the suitability of the swelling and collapse theory proposed based on the virgin compression surface (VCS). It is important to identify whether the developed modified MPK framework is valid when the experimental results of independent studies from the literature are utilized. Previous studies that investigated swelling and collapse potential were carried out based on one-dimensional consolidation tests under controlled suction conditions. In the current study, standard Proctor compaction and one-dimensional (1-D) swell tests were performed to measure the Optimum Lime Content (OLC) according to swelling potential. The virgin compression surfaces were generated by conducting static compaction tests at various net stresses and a relationship between moisture ratio and the net stress was proposed. Next, 1-D compression and consolidation laboratory tests were carried out and the results were used to investigate and compare the mechanism of collapse and swelling based on suction-based theory such as Alonso et al. (1990) model and moisture content-based theory such as the modified MPK framework. The shape of Loading-Collapse for the untreated and lime-treated clays was also studied based on Alonso et al. (1990) model. For further validation of the modified MPK framework, the results obtained by Jotisankasa et al. (2007) under controlled suction testing were incorporated into the modified MPK framework and discussed. By verifying the suitability of the theory of swelling and collapse proposed based on the developed VCS, it is a straightforward procedure to predict the collapse for any stress and moisture state and to recognize the specimen behavior, in terms of swell or collapse, after wetting. This meets the industry's requirement and practice where the preference is toward using the conventional parameters including moisture content, void ratio and stress and avoiding measuring the suction parameter which requires special equipment and expertise.

2. Material and methodology

The expansive clay chosen in this research was a Quaternary age basaltic residual subgrade widely spread across Western Victoria, Australia (McAndrew and Marsden, 1973). The soil was collected from a depth of 2 m below the ground. This was the same geology formation from which soils samples were previously utilized to propose the swelling and collapse theory based on VCS developed within the modified MPK framework (Al-Taie et al., 2019). The specific gravity of the soil was obtained following the ASTM-D854 (2010) procedure to be 2.71. Based on the ASTM-D422 (2007), sand content was found to be 4%, and fine (silt and clay) content was 96%. The linear shrinkage, liquid limit, plastic limit and plasticity index of the soil were 20.3%, 73.7%, 23.2% and 50.5%, respectively, following AS1289.3.4.1 (2008) and ASTM-D4318 (2000). The selected soil was categorized as clay with high plasticity based on ASTM-D2487 (2011).

To study the suitability of the modified MPK for the incorporation of the swelling and collapse theory, a series of laboratory tests were carried out. First, standard Proctor compaction and one-dimensional swell tests were carried out to measure the OLC according to the swelling reduction. Second, samples were compacted statically to generate the VCS. Next, the relationship between the moisture ratio and the net stress was proposed. The mechanisms of collapse and swelling were investigated based on Alonso et al. (1990) model and Modified MPK framework using the obtained 1-D compression and consolidation laboratory tests. The shape of Loading-Collapse (stress-suction relationship) for the untreated and lime-treated clays was also studied. Finally, the developed VCS was further validated by utilizing the experimental results presented by Jotisankasa et al. (2007) to the modified MPK framework. The following sections describe the experimental procedures carried out in this research.

2.1. Determination of the optimum lime content

The standard Proctor compaction test was performed according to ASTM-D698 (2012) to measure the optimum moisture content (OMC) and maximum dry density (MDD) for the untreated clay samples. Dry clay was thoroughly mixed with various moisture contents and left for 7 days for equilibrium. Measuring the moisture contents at different locations of the sample after 7 days showed a difference of less than 0.5%. For lime-treated samples, the compaction technique presented by Ciancio et al. (2014) was followed. Distilled water was added to the mixture of the dry clay and lime at 2%, 3%, 4%, 6%, and 8% lime contents. The mixtures were left for one hour and the compaction test was then conducted. The same approach was followed for different moisture and lime contents.

One-dimensional swell tests were carried out to determine the OLC. The specimens were prepared at optimum moisture content and maximum dry density (Table 1). The lime-treated specimens were left for curing for 1, 7 and 28 days at a controlled temperature of 20 ± 2 °C and the relative humidity of 95% to identify the period required for a significant reduction in swelling potential. The specimens were mounted in the oedometer frame and then inundated under a surcharge of 25 kPa to compensate for the field stress conditions from which the sample had been collected.

2.2. Establishment of the virgin compression surface

Static compaction set up for establishing the VCS is shown in Fig. 3. Static compaction tests were conducted on untreated and lime-treated basaltic expansive clay to develop a group of compaction curves. The specimens were compressed statically under stress levels ranging from 2 kPa to 4000 kPa and with moisture contents ranging from 0% to 50%. The stress of 2 kPa was, in fact, the stress of the loading cap weight.

For the untreated clay, various amounts of water were added to the mixture of dry clay and lime. The mixtures were left for 7 days to allow thorough permeation of the water throughout the mixtures. The specimens were then compacted statically into the mold with a sealed base.

During the loading phase, the rate of stress increments was selected to assure that the excess air pressure does not increase during loading (Table 2). For specimens prepared at the dry side of the Line of Optimums (LOO), as the air is easy to release under high-stress rates, it can be supposed that excess air pressure does not increase during loading. LOO was drawn by connecting the point on each e-ew curve from where no more decrease in void ratio occurs. Once the water content of samples reached the LOO, the stress rate was decreased to build the drained paths averting excess air pressure to increase. Several drained constant net stress contours between the LOO and saturation line [normally consolidated line (NCL)] were developed to establish the VCS contours. To develop a drained constant net stress contour, specimens at different moisture contents were compressed. Once the moisture content reached the LOO, a much slower stress rate was applied assuring no pore air pressure builds up in the sample. According to these developed constant net stress contours, the specimens at the dry and wet side of the LOO were compacted at stress rates shown in Table 2. Finally, the void ratios were measured and consequently, the VCS for the untreated clay was established.

The same procedure was followed to establish the surface for the lime-stabilized samples except that the stress rates were greater than those of untreated samples when the water contents reached the LOO, as shown in Table 2.

Table 1
OMC, MDD, and swelling values of untreated and lime-treated samples.

Lime (%)	OMC (%)	MDD (kN/m^3)	Swelling after curing (%)			
			0 day	1 day	7 days	28 days
0	25	14.9	6.3			
2	26	14.78		3.3	2.7	2.5
3	26.5	14.68		2.4	1.87	1.68
4	26.9	14.61		0.4	0	0
6	27.8	14.54		0	0	0
8	28.5	14.41		0	0	0

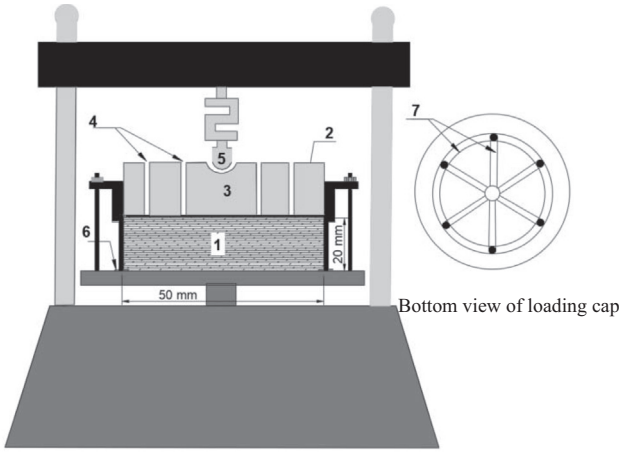

1: Sample, 2: Filter paper, 3: Loading cap, 4: Holes (2 mm)
5: Loading shaft, 6: Plastic O-rings, 7: Channels

Fig. 3. Set-up of static compaction.

This was due to the fact that the stabilization process initiated once the water was added.

2.3. Measurement of preconsolidation pressure for unsaturated and saturated clays

To study the mechanism of collapse and swelling of untreated and lime-treated specimens based on Alonso et al. (1990) model, the preconsolidation pressures for unsaturated and saturated specimens were obtained. To achieve this target, two untreated and two lime-treated specimens were statically compacted to 300 kPa under a constant moisture content of 20% ($e_w = 0.542$).

The preconsolidation pressure of one of the two untreated or lime-treated specimen was identified by subjecting it to constant incremental pressures ranging from 2 to 1800 kPa and recording the settlement. During the test, the oedometer cell was covered with plastic wrap to avoid moisture loss. After plotting the data in the e-log (σ) plane, the preconsolidation pressure for the unsaturated specimen was obtained. The second untreated or lime-treated specimen was compacted under the net stress of 300 kPa and a constant moisture content of 20% and was inundated with distilled water under the stress of 2 kPa. Following that, the specimen was subjected to different constant vertical stresses every 24 h (ASTM-D2435, 1996). By plotting the data in the e-log(σ) plane, the preconsolidation pressure for saturated soil was obtained.

2.4. Determination of suction

The Loading-Collapse (LC) is defined as the relationship between stress (σ) and suction (s) at constant void ratio (e). In order to study the shape of Loading-Collapse for the untreated and lime-treated clays, it was necessary to measure the suction. The values of suction in different moisture contents were measured by using the Hyprop or Chilled Mirror Hygrometer (WP4C) device. The relationship between moisture content and suction is described as the Soil Water Characteristic Curve (SWCC). The SWCC is also used to estimate engineering properties of the soil, such as unsaturated hydraulic conductivity, compressibility, shear strength and swelling potential of fine-grained soils (Rao et al., 2011; Singh and Kuriyan, 2003; Tarantino et al., 2008).

The Hyprop uses tensiometers and measures the matric suction of soils within a range of 0–1.5 MPa which is corresponding to relatively high moisture contents (Murray and Sivakumar, 2010; UMS, 2013). However, the WP4C relies on the Chilled Mirror dewpoint technique, which measures the total suction (i.e. the sum of matric suction and osmotic suction) of soils within a range of 1.5–

Table 2
Stress rates applied to compact untreated and lime-treated clays.

Soil type	Compaction stress (kPa)	Stress rate (kPa/min)	
		Dry side of LOO	Wet side of LOO
Untreated clay	≤1000	20	0.5
	>1000	100	1.5
Lime-treated clay	≤1000	20	4
	>1000	100	8

60 MPa, corresponding to relatively low moisture contents (ASTM-D6836, 2016). As the suction in LC relation is usually expressed in terms of matric suction, the total suction obtained by WP4C was converted to the matric suction. This was achieved by measuring the osmotic suction using the filter paper technique following ASTM-D5298 (2016).

3. Experimental results

3.1. Determination of the optimum lime content

The compaction and 1-D swell test results for untreated and lime-treated samples are presented in Table 1. The swell test results suggest a considerable decrease in swelling potential after the addition of 2% lime and the swelling amount became zero after the addition of 4% lime. Results also indicate that the reduction in swelling potential within the first 7 days is greater than that between the 7th and 28th day of curing. Based on the results, the OLC of the expansive clay of this research was 4%.

3.2. Development of the virgin compression surfaces

The procedure described in the Methodology section was followed to develop the virgin compression surface (VCS) for the untreated and 4% lime-treated clays as presented in Figs. 4 and 5. The VCS represented the loosest state of a compacted soil at any specific net stress and moisture ratio. Figs. 4 and 5 show that the moisture ratio decreased as the void ratio increased. This occurred for all untreated and lime-treated specimens prepared at a moisture ratio of e_w and compacted to reach a void ratio of e which is corresponding to a degree of saturation higher than 37% and 33%, respectively. For very dry soils with a degree of saturation less than 37% and 33% for untreated and lime-treated specimens, respectively, the moisture ratio increased with an increasing void ratio. This is due to the weakening of the effect of suction in generating strong contact between particles and hence larger macro void space can be formed.

3.3. Relationship between moisture ratio and net stress

The VCS represents the yield positions at which plastic collapse occurs during loading and wetting or reloading and wetting. Loading-Collapse (LC) curve is one of the key yield loci that describes where plastic collapse could take place during wetting. The LC determines the relation-

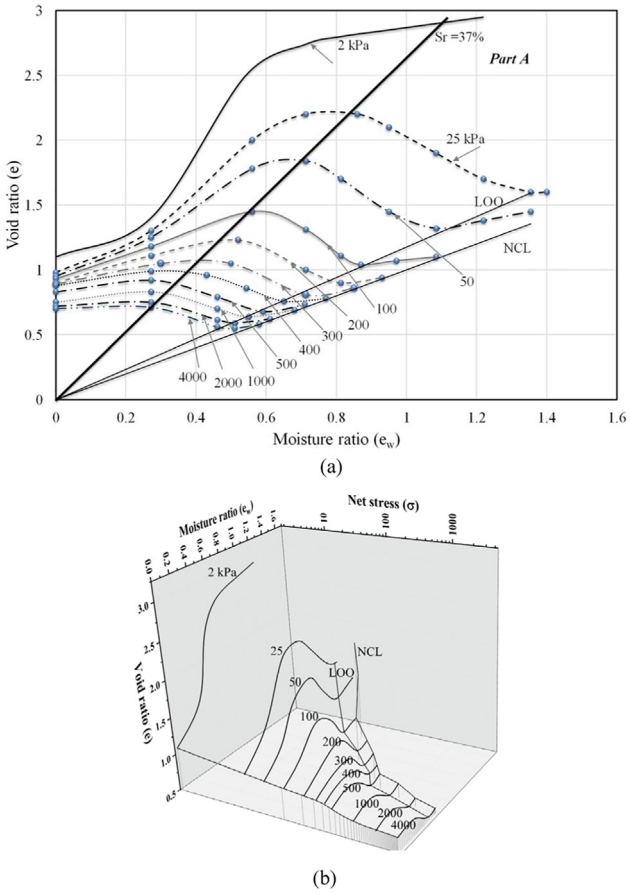

Fig. 4. Virgin compression surface for the expansive clay in (a) e-e_w (b) e-e_w-log (σ) space.

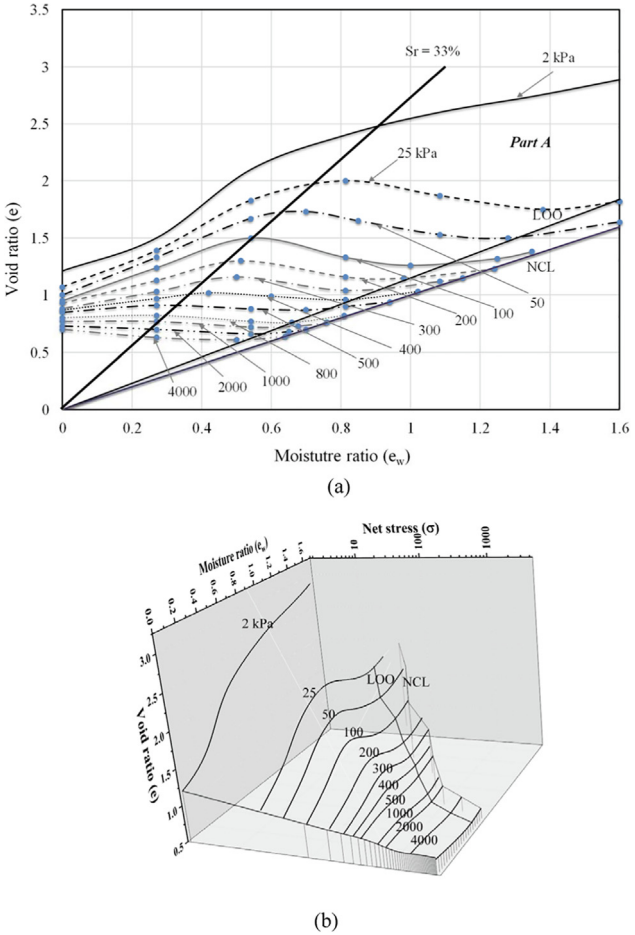

Fig. 5. Virgin compression surface for the lime-treated clay in (a) e-e_w (b) e-e_w-log (σ) space.

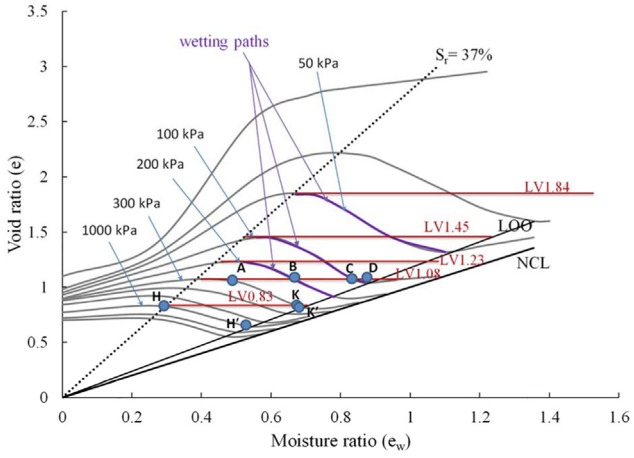

Fig. 6. Constant void ratio lines on the VCS (untreated clay).

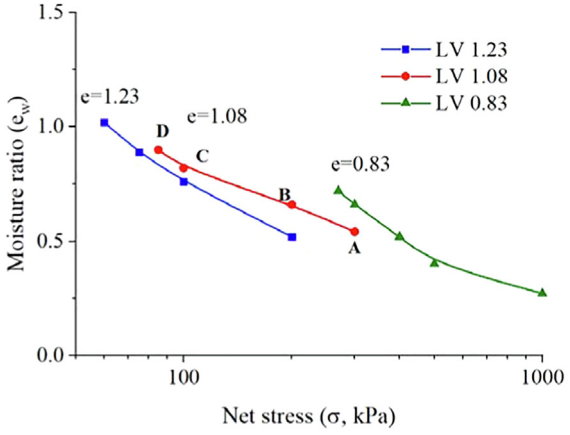

Fig. 7. Relationship between e_w and σ at constant e (untreated clay).

ship between suction (s) and net stress (σ) at a constant void ratio. This relationship describes the hardening, yielding and collapse of compacted soil (Alonso et al., 1990).

The MPK framework considers moisture ratio as the main state variable; hence, it is important to establish a relationship between e_w and σ at constant void ratios for both untreated and lime-treated clays.

To achieve the relationship between e_w and σ for the untreated clay using the VCS, the surface in the e-e_w space was divided into several horizontal lines (constant void ratio lines, LV), as shown in Fig. 6. As indicated in Fig. 2, the wetting paths follow the MPK framework (Part A); however, the MPK framework is not applicable to specimens prepared at a degree of saturation less than 37% and compressed under stress levels less than 1000 kPa. Fig. 6 shows that the maximum decrease in the void ratio occurred when the wetting path reached the LOO. Therefore, the constant void ratio lines (LVs) were drawn from the highest void ratio of each stress contour to the LOO. For each LV in Fig. 6, the moisture ratio-net stress relationship could be obtained as plotted for LVs of 0.83, 1.08 and 1.23 and presented in Fig. 7. For instance, for the LV1.08 in Fig. 6, all points generated by the intersection between the LV1.08 and the stress contours of 300, 200, 100 and 85 kPa (estimated between 100 kPa and 50 kPa stress contours) could be plotted in terms of the moisture ratio and net stress. The intersection points A, B, C and D are shown in Figs. 6 and 7.

Similarly, for the lime-treated clay, the VCS in the e-e_w space was divided into several LVs, as presented in Fig. 8. The wetting paths follow the MPK framework (Part A); however, the MPK framework does not apply to specimens prepared at a degree of saturation less than 33% and compressed under stress levels less than 500 kPa. For the selected LVs of 0.78, 1.17 and 1.33 from Fig. 8, the moisture ratio-net stress relationship was obtained and demonstrated in Fig. 9. The LV1.17 in Fig. 8, for example, includes the stress contours of 300, 200 and 185 kPa (estimated between 200 kPa and 100 kPa stress contours). All points established by the intersection between the LV1.17 and the stress contours of 300, 200 and 185 kPa could be

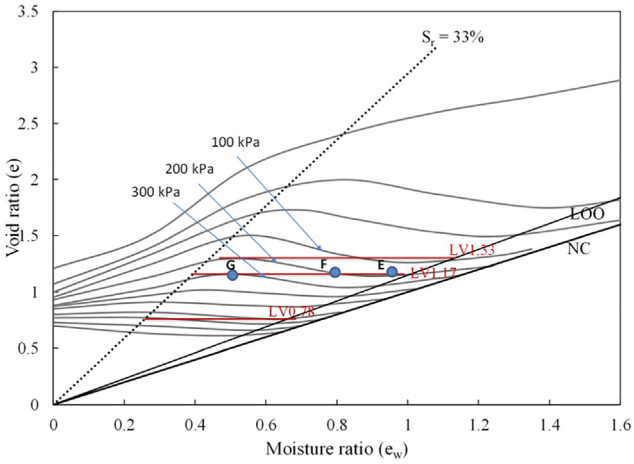

Fig. 8. Constant void ratio lines on the VCS (lime-treated clay).

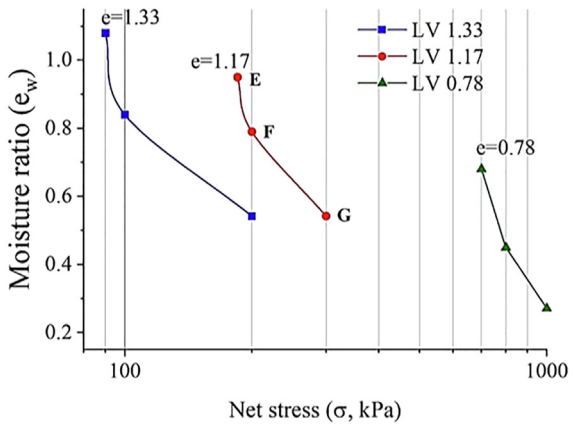

Fig. 9. Relationship between e_w and σ at constant e (lime-treated clay).

plotted in terms of moisture ratio and net stress. The intersection points E, F, and G are also shown in Figs. 8 and 9.

3.4. Selection of Alonso et al. (1990) model to evaluate the mechanism of collapse and swelling

Alonso et al. (1990) model was selected as a widespread accepted suction-based theory to evaluate the mechanism of collapse and swelling based on the modified MPK framework which is a moisture content-based approach. Alonso model was intended for unsaturated soils which are slightly or moderately expansive. The question raised here is whether this model could be utilized to evaluate the collapse and swelling mechanism based on the constitutive virgin compression surface (VCS) developed in the modified MPK framework. The method proposed by Al-Taie et al. (2019) could predict the state of a specimen after wetting in terms of collapse and swelling based on the VCS. Regarding the collapse, this method not only could predict the state of the specimen but also the magnitude of collapse. For swelling, this method could only predict the state of the specimen after wetting and the value of swelling depended on the gradient of swelling. This means that the major objective of this method was defining the collapse domain starting from zero to the maximum value. For example, the specimen H in Fig. 6 compacted to the stress of 1000 kPa under a constant moisture content of 10% (e_w = 0.271) and then wetted under the stress of 300 kPa (the last stress contour located at the LV0.83) collapsed to follow the path of KK′ (collapse is approximately zero). However, if the specimen H was wetted under a stress equivalent to the compaction stress (1000 kPa in Fig. 6), the specimen collapsed to follow the path of HH′ (maximum collapse). Therefore, the experimental results of this research and the Alonso et al. (1990) model were utilized to focus on the range of the collapse and limited values of swelling where the application of this model was still valid.

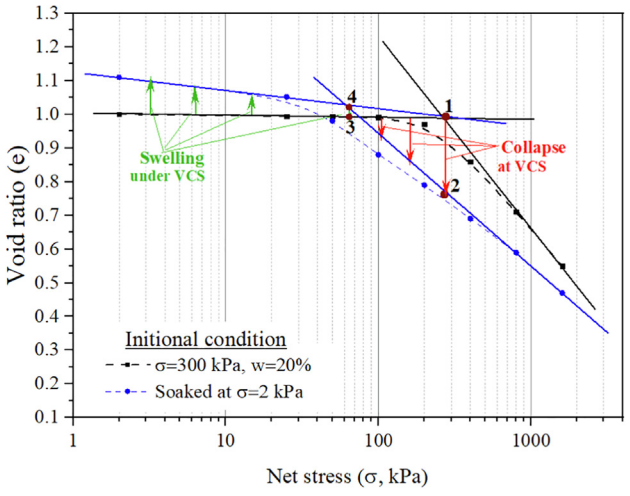

Fig. 10. Collapse and swelling mechanism for untreated soil.

3.5. Collapse and swelling mechanism in terms of Alonso et al. (1990) model and modified MPK framework

The Alonso et al. (1990) model used the net stress and suction as independent stress state variables. The results of many suction-controlled laboratory tests carried out on compacted kaolin and a sandy clay were used to derive the location of yield points. To allocate the yield points, Alonso et al. (1990) identified the preconsolidation stresses for two specimens loaded, unloaded, and reloaded at different suction values. In this research, to investigate the mechanism of collapse and swelling based on Alonso et al. (1990) model and modified MPK framework, two untreated and two lime-treated specimens were compacted statically to 300 kPa under a constant moisture content of 20% (e_w = 0.542). The moisture content of 20% is corresponding to the degree of saturation of 50% and 46% for the untreated and lime-treated clays, respectively.

The preconsolidation pressure for the first unsaturated specimen, compacted statically to 300 kPa under a constant moisture content of 20% (e_w = 0.542), was obtained to be approximately 280 kPa (point 1 in Fig. 10), which was close to the compaction pressure of 300 kPa. In this constant moisture content compression test, the degree of saturation changed from 50% to 98% at the end of the test. The second specimen was compacted statically to 300 kPa under a constant moisture content of 20% and then soaked with distilled water under the stress of 2 kPa and the preconsolidation pressure was approximately 63 kPa (point 4 in Fig. 10).

To investigate the mechanism of swelling and collapse based on Alonso et al. (1990) model for untreated soil, it is important to identify the conditions at which the specimen could swell or collapse after wetting. Fig. 10 shows that if a specimen was compacted statically to 300 kPa under a constant moisture content of 20% (point 1) and then wetted to the saturation condition under the stress of 280 kPa (compaction pressure), it would collapse and follow the path from point 1 to point 2. However, if the specimen at point 1 in Fig. 10 was unloaded to a stress equivalent to the preconsolidation pressure of saturated soil (63 kPa), the specimen would swell (i.e. no additional collapse) and would follow the path from point 3 to point 4, as shown in Fig. 10.

For the lime-treated clay, the same approach was followed to measure the preconsolidation pressure. The preconsolidation pressure for the first specimen, compacted statically to 300 kPa under a constant moisture content of 20%, was found to be 310 (point 5 in Fig. 11), which was relatively close to 300 kPa (compaction stress). During the constant moisture content compression test, the degree of saturation increased from 46% to 73% at the end of the test. The preconsolidation pressure for the second specimen, compacted statically to 300 kPa under a constant moisture content of 20% and then soaked with distilled water under the stress of 2 kPa, was found to be 165 kPa (point 8 in Fig. 11). By focusing on the mechanism of col-

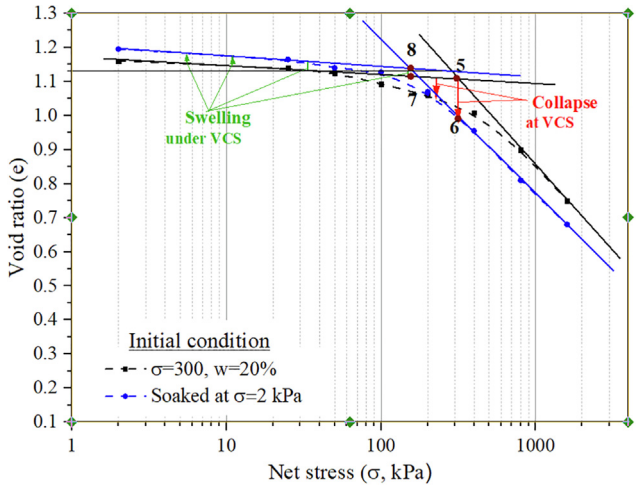

Fig. 11. Collapse and swelling mechanism for lime-treated soil.

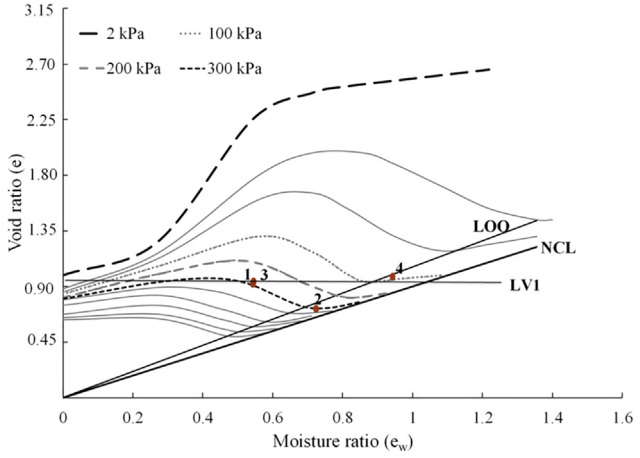

Fig. 12. Mechanism of collapse and swelling according to the modified MPK framework (untreated soil).

lapse and swelling for lime-treated soil in Fig. 11, it is expected that if a specimen was compacted statically to 300 kPa under a constant moisture content of 20% (point 5) and then wetted to the saturation condition under the stress of 310 kPa (compaction pressure), it would collapse and follow the path from 5 to 6 (Fig. 11). However, if the specimen at point 5 was unloaded to a stress equivalent to the preconsolidation pressure of saturated soil (165 kPa), the specimen would swell and follow the path from 7 to 8 (Fig. 11).

To reflect the points in Figs. 10 and 11 onto the modified MPK framework, a new equivalent plot was developed, as shown in Figs. 12 and 13. For untreated soil (Fig. 12), the constant void ratio line (LV) needed to be plotted on the VCS. This could be achieved by determining the moisture ratio, compaction stress and the corresponding void ratio of the specimen after compaction. As the specimen was prepared at the moisture content of 20% (e_w = 0.542) and compacted to the stress of 300 kPa and the corresponding void ratio after compaction was 1 (see Fig. 10), the first yield point (e,e_w,σ) on the modified MPK framework was found to be (1, 0.542, 300) (point 1 in Fig. 12). From point 1, a horizontal line was plotted to represent the LV1. The stress contours of 300 kPa, 200 kPa, and 100 kPa located at the LV1. As the modified MPK framework suggested that specimens wetted under a stress located at the LV would collapse after wetting, it was expected that the specimen at point 1 collapsed to follow the path from 1 to 2 in Fig. 12. If the specimen at point 1 was unloaded to the stress of 63 kPa, the path moved inside the VCS and followed the path from 1 to 3 in Fig. 12. As the stress of 63 kPa was above the LV1, it was expected that the specimen at point 3 swelled after wetting under the stress of 63 kPa. The same procedure was followed for the lime-treated soil as shown in Fig. 13. From Figs. 10–13, a new method can be suggested to identify the collapse/swelling behavior of the specimen after wetting. This method does not require the virgin compression surface to be established; rather it depends on determining the initial state of the specimen after compaction (moisture content, void ratio, and corresponding preconsolidation pressure) and preconsolidation pressure for a saturated sample. This method can be summarized as follows:

1. The initial state of the specimen should be identified (moisture content, void ratio and preconsolidation pressure (Pc_1)),
2. An identical specimen requires to be saturated under a very small vertical stress (e.g. 2 kPa) and subsequently, the preconsolidation pressure of the saturated soil (Pc_2) is obtained,
3. If a specimen was prepared at the initial state and then wetted under a stress level (Pc) between Pc_1 and Pc_2 ($Pc_2 < Pc \leq Pc_1$), the specimen collapses,

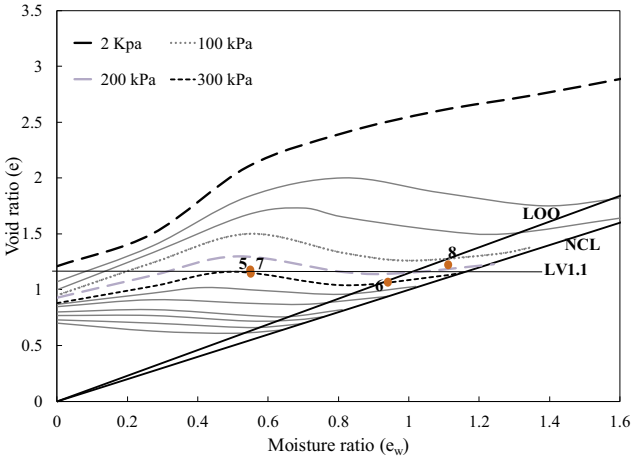

Fig. 13. Mechanism of collapse and swelling according to the modified MPK framework (lime-treated soil).

4. However, for a specimen prepared at the initial state and then wetted under a stress level lower than the preconsolidation pressure of the saturated soil Pc_2 ($Pc \leq Pc_2$),

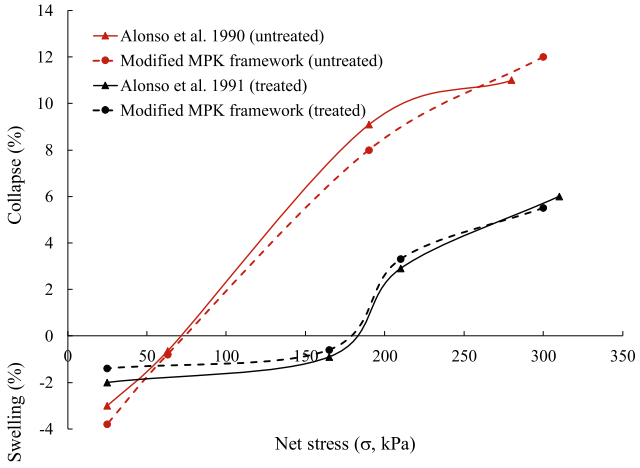

Fig. 14. Collapse and swelling potentials for untreated and lime-treated soil according to Alonso et al. (1990) model and the modified MPK models.

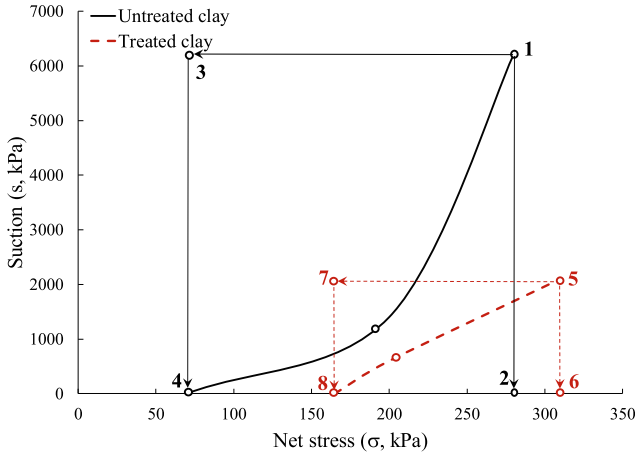

Fig. 15. Yield curves for untreated and lime-treated soils in σ-s space.

the specimen swells.

To compare the collapse and swelling potential according to the Alonso et al. (1990) model and the modified MPK framework, Fig. 14 was plotted. Fig. 14 shows that the modified MPK framework interpreted collapse and swelling values that were close to the results obtained using the Alonso et al. (1990) model.

3.6. Loading-collapse shape for untreated and lime-treated clays

To investigate the σ vs s behavior of the untreated samples at a constant e, the values of suction at points 1 and 4 in Figs. 10 and 12 were measured. Using the filter paper technique, the osmotic suction for the untreated soil was measured and found to vary from 80 kPa to 100 kPa. The matric suction for the specimen at point 1 was measured to be 6200 kPa as shown in Fig. 15. As specimen at point 4 was in saturation condition, the matric suction was expected to be approximately zero. As relationship between σ and s is normally represented by a curve, at least a third point was needed to be obtained. The third specimen was initially compacted to 300 kPa at a moisture content of 20%, then wetted to a moisture content of 24% under a stress of 2 kPa. The specimen was covered with plastic wrap and left for 24 h to equilibrate. The preconsolidation pressure of the unsaturated sample was determined to be 190 kPa. The matric suction of the third specimen was measured to be 1150 kPa. Fig. 15 presents the behavior of the untreated soil (Loading-Collapse) in the σ-s space as a curve, which is consistent with the shape and evolution of the yield curve proposed by Alonso et al. (1990) and the LC curve in Fig. 17c.

To study the behavior of lime-treated soil in the σ-s plane, the values of suction were measured for specimens at points 5 and 8 (Figs. 11 and 13). The osmotic suction for the lime-treated varied from 340 to 380 kPa. The matric suctions for the specimens at points 5 and 7 were measured to be 2100 kPa and zero as shown in Fig. 15. A third specimen was initially compacted to 300 kPa at a moisture content of 20%, then wetted to a moisture content of 29.5%, under the net stress of 2 kPa. The specimen was covered with plastic wrap and left for 4–8 h for equilibrium and was then cured for 7 days. As the moisture content of the specimen was 29.5%, the degree of saturation was approximately 70%, the specimen had a moisture ratio-void ratio state close to the LOO. The preconsolidation pressure in this sample was 210 kPa. The matric suction of 650 kPa was measured for the third specimen. From Fig. 15, it can be noticed that the Loading-Collapse behavior of stabilized soil in σ-s space can be represented as a line.

Fig. 15 also shows that the Loading-Collapse path for the untreated soil involved a range of suction starting from 0 to 6200 kPa; however, this path involved a range of suc-

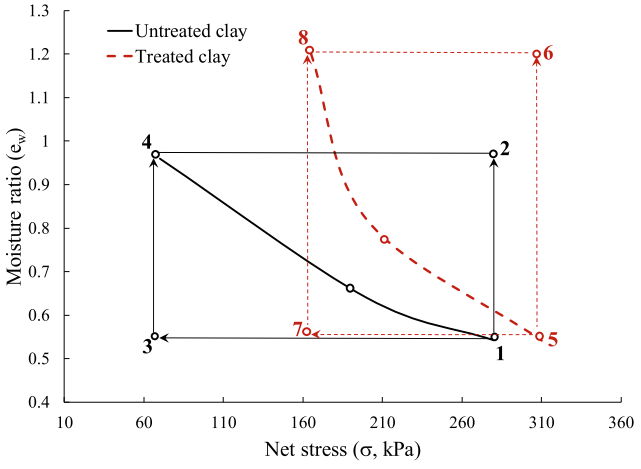

Fig. 16. Yield curves for the untreated and lime-treated soils in σ-e_w space.

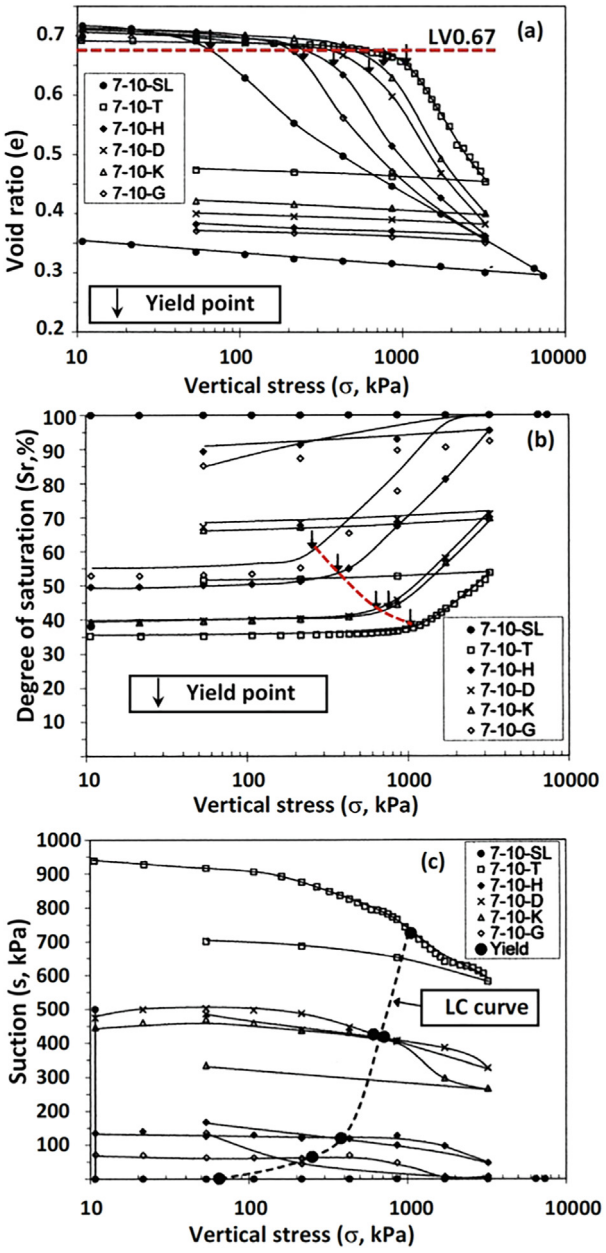

Fig. 17. Results of loading tests under constant moisture content for series 1 (after Jotisankasa et al. (2007)).

tion starting from 0 to 2100 kPa for the lime-treated soil. This showed that the Loading-Collapse path for the untreated soil occurred at a range of suction wider than that for the lime-treated soil.

The modified MPK framework considers the moisture content as the main state variable as an alternative to suction. Hence, the plot of Fig. 15 in σ-s plane was converted to the plot presented in Fig. 16 in a σ-e_w plane. Curves demonstrated in Fig. 16 are consistent with the shape and development of the yield curves presented in Figs. 7 and 9.

3.7. Evaluation of the modified MPK framework using Jotisankasa et al. (2007) results

The study of Jotisankasa et al. (2007) investigated the collapse behavior of an unsaturated soil using a suction-monitored oedometer test. Their experimental results were chosen as an example of a study that utilized suction-monitored testing to investigate the concept of LV using the modified MPK framework. Jotisankasa et al. (2007) investigated the collapse behavior of an unsaturated soil using a suction-monitored oedometer test. The soil used in their study was a mixture of 70% silt, 20% kaolin and 10% London clay. A modified oedometer (Ridley and Burland, 1993) was used to monitor the changes in suction using suction probes during loading and wetting.

The specimens were compacted using a static method inside the oedometer cell. The initial properties of the specimen selected to be investigated in this research (series 1 specimens as indicated in Jotisankasa et al. (2007)) are presented in Table 3. The corresponding testing program for the selected specimens is presented in Table 4. The regime included three groups of specimens, being A, B and C. Group **A** involved a specimen, saturated under vertical stress of 11 kPa, compressed in a fully saturated condition to 7336 kPa, and then unloaded to 11 kPa. Groups **B** included the loading of specimens under a constant moisture content to particular compaction stress and then unloading to certain stress. Group **C** involved wetting specimens at a constant stress level to achieve collapse.

The results of Groups **A** and **B** are presented in terms of specific volume ($1 + e$), the degree of saturation, suction, and net stress. However, to serve our study, the specific volumes were converted to void ratios (Fig. 17a). Fig. 17a presents the values of yield points (preconsolidation pressure) for specimens compressed at various degrees of saturation. It is clear that the yield points of all specimens occurred at approximately the same void ratio value of 0.67. To apply this state to the modified MPK framework, an average line connecting the yield points (LV 0.67) was plotted as indicated in Fig. 17a. This line can be obtained from two methods. First, by loading specimens prepared at various initial moisture contents to different compaction stresses. The obtained void ratio values are approximately the same after loading. Second, specimens are compressed to the same stress level under a constant moisture content and then wetted to different moisture contents. After wetting, the

Table 3
Initial properties of the test series studied by Jotisankasa et al. (2007).

Series	Specific volume ($1 + e$)	Moisture content (%)	Degree of saturation (%)	Initial suction (kPa)
1	1.7	10.2	38	475 ± 15

Table 4
Testing program for test series 1 (Jotisankasa et al., 2007).

Group	Test	State paths followed after compaction
A	1-SL	Soaked at 11 kPa/loading to 7336 kPa/unloading to 11 kPa
B	1-D	W (10.6%)/L (3220)/U (54)
	1-G	W (14.8%)/L (3220)/U (54)
	1-H	W (13.5%)/L (3220)/U (54)
	1-K	L (3220)/U (54)
	1-T	D (9.2%)/L (3220)/U (54)
C	1-I	L (430)/W (130 kPa)/L (3220)/U (54)
	1-J	L (215)/W (50 kPa)/L (861)/U (54)
	1-N	L (108)/W (10 kPa)/U (54)
	1-Q	L (594)/W (40 kPa)/U (54)

W: wetting to x% MC, or to x kPa suction at constant vertical stress.
L: loading to x kPa at constant MC.
U: unloading to x kPa at constant MC.
D: drying to x% MC at zero vertical stress.
MC: moisture content.

preconsolidation pressure (yield points) values are obtained and connected by a line, i.e., LV as defined above.

In this study, the LV was drawn according to the second method described above based on the experimental test results of Jotisankasa et al. (2007). Fig. 17a clearly indicates that the average line that connected the yield points were located at a constant void ratio of 0.67 (LV0.67). This line can be presented within the modified MPK framework as shown in Fig. 18a.

To interpret the experimental results of Jotisankasa et al. (2007) using the modified MPK framework, first, the initial properties of the specimens (after compaction) were identified. These properties included moisture content, preconsolidation pressure (yield point), and corresponding void ratio. As presented in Table 3, the moisture content of the specimen was 10.2% ($e_w = 0.266$, where $G_s = 2.61$). The 1-K test given in Table 4 (Group **B**) and shown in Fig. 17a represented the e-log(σ) relationship for a specimen immediately after compaction (initial condition). As shown in Fig. 17a, the preconsolidation pressure was approximately 750 kPa, with a corresponding void ratio of 0.66. At this stage, based on Fig. 18, the first yield point on the modified MPK framework (e,e_w,σ) was identified (0.66, 0.266, 750). All specimens in the five tests of Group B presented in Table 4 were compressed at a moisture content of 10.2% to the stress level of 750 kPa, and then different state paths were performed to achieve a specific target.

Using the results of Group **B**, the preconsolidation pressures at various moisture contents were obtained. For example, for the 1-H specimen prepared at a moisture content of 10.2% and compressed to the stress level of 750 kPa, then wetted to the moisture content of 13.5% ($e_w = 0.352$), the preconsolidation pressure was 400 kPa, with a void ratio of 0.66. Consequently, the second yield point on the modified MPK framework was found to be (0.66, 0.352, 400) as presented in Fig. 18. For the 1-T specimen with 10.2% moisture content compressed to the stress level of 750 kPa and then dried to the moisture content of 9.2% ($e_w = 0.240$), the preconsolidation pressure was 1000 kPa, with a void ratio of 0.67. Therefore, another point was found to be (0.67, 0.240, 1000). The same procedure was followed to find the preconsolidation pressures of 1-G specimen in Group B and 1-SL specimen in Group A, as shown in Table 5. After plotting these points, an average horizontal line was drawn to pass through them. This line intersected the void ratio axis at a value of 0.67 (LV0.67). Therefore, as illustrated in Fig. 18, the LV0.67 intersected the stress contours of 65, 250, 400, 750, and 1000 kPa at points of ($e_w = 0.68$, $e = 0.67$), ($e_w = 0.386$, $e = 0.67$), ($e_w = 0.352$, $e = 0.67$), ($e_w = 0.266$, $e = 0.67$), and ($e_w = 0.24$, $e = 0.67$), respectively. According to the studies of Tripathy et al. (2002) and Islam (2015), the LOO line was assumed to occur at a degree of saturation of 85%. Therefore, the LOO was plotted at a degree of saturation of 85%.

Fig. 17b shows the relationship between the degree of saturation and net vertical stress. If the yield points are connected using a curved line, as shown in Fig. 17b, a relationship between the degree of saturation and net stress can be obtained. To find the relationship between moisture ratio and net stress, the equivalent moisture ratios at yield points were measured according to the data presented in Fig. 17b. Fig. 19 presents the relationship between moisture ratio and net stress at yield points and aligns with the results obtained from this research (Figs. 7 and 9).

The results of Group **C** tests induced collapse potential due to wetting as shown in Fig. 20. To represent these results within the modified MPK framework, two tests were selected, being 1-Q and 1-I. The state paths of these tests included loading to the stresses of 594 and 430, respectively. Therefore, it was important to find the intersection points (yield points) between the LV0.67 and the stress contours of 594 kPa and 430 kPa. The yield points (points **b** and **e** in Fig. 18a) were allocated according to the data presented in Fig. 17b. For the 1-Q test, the specimen with

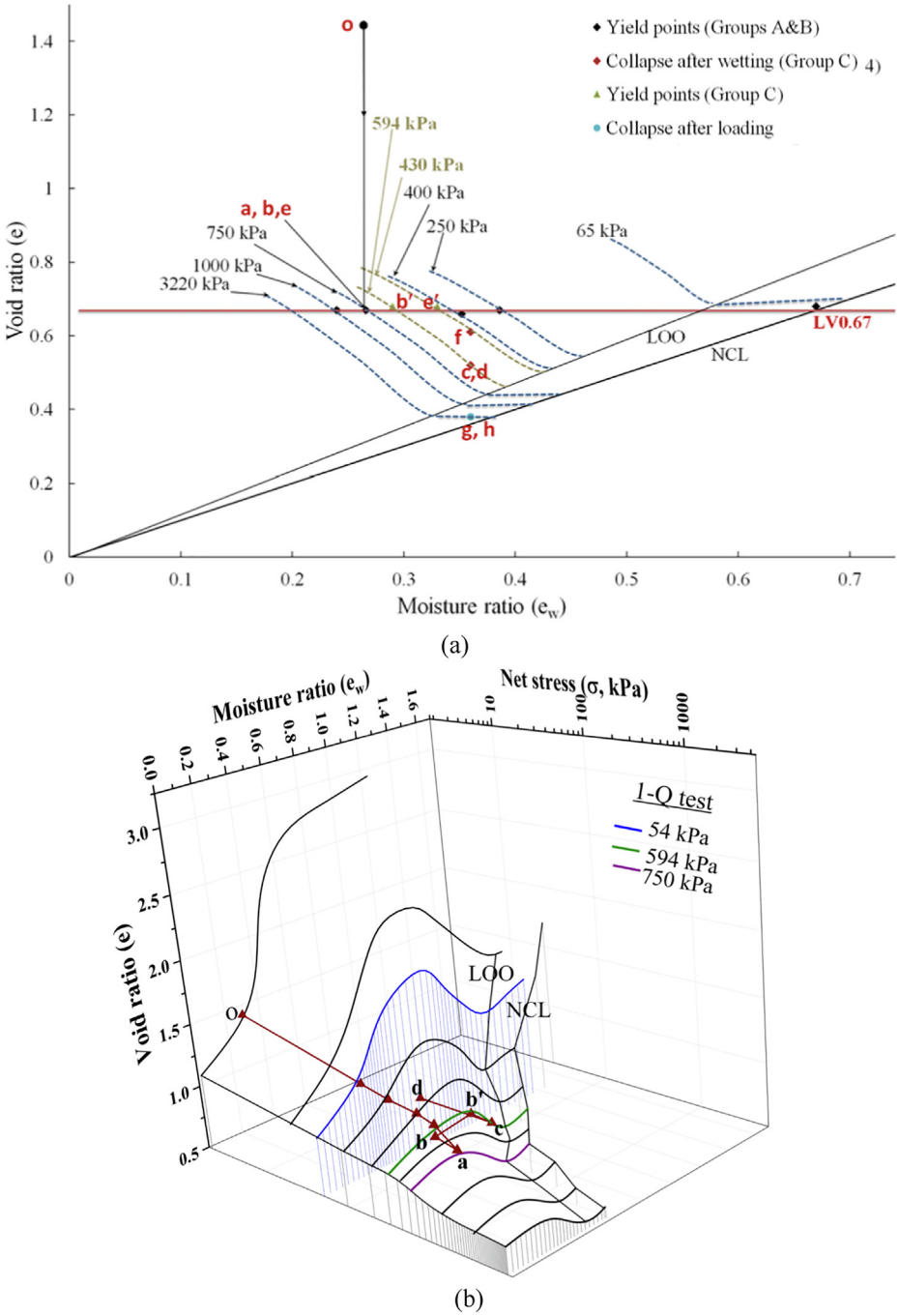

Fig. 18. Results of Groups A, B and C in terms of void ratio, moisture ratio and net stress.

Table 5
Preconsolidation pressures and corresponding moisture content and void ratio for specimens in Group A & B.

Group	Test	(e, e_w, σ)
A	1-SL	(0.68, 0.68, 65)
B	1-D	(0.65, 0.276, 650)
	1-G	(0.66, 0.386, 250)
	1-H	(0.66, 0.352, 400)
	1-K	(0.66, 0.266, 750)
	1-T	(0.67, 0.240, 1000)

10.2% moisture content was compressed to the stress of 750 kPa at the VCS (point **a** in Fig. 18a and b). The specimen was then unloaded to 594 kPa and the path moved below the surface (the path of **ab** in Fig. 18a and b). After wetting, the specimen swelled; however, the amount of swelling was negligible (swelling <0.3%). The swelling path hit the surface at point **b′** to follow the path of **bb′** as presented in Fig. 18a and 18b. With continuous wetting, the specimen collapsed to follow the path of **b′c** on the VCS. The specimen was then unloaded to 54 kPa and followed

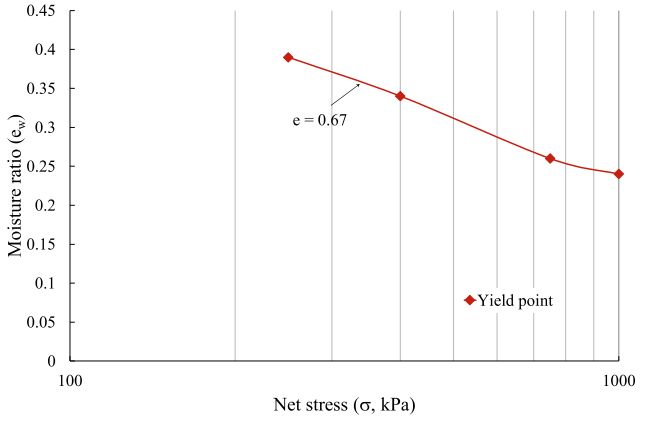

Fig. 19. Relationship of e_w and σ at constant e based on Jotisankasa et al. (2007) results.

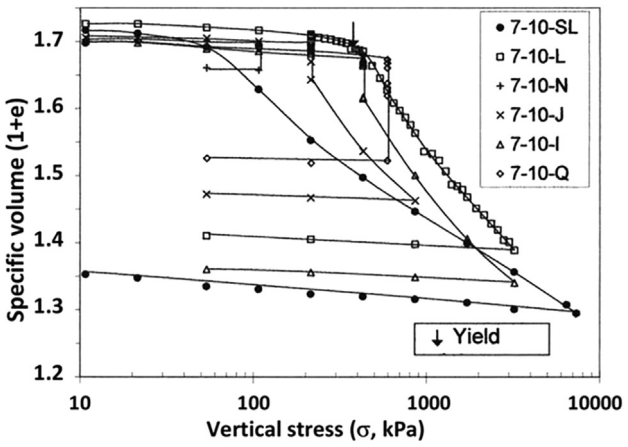

Fig. 20. Results of Group 4 tests induced collapse due to wetting (Jotisankasa et al., 2007).

the path of **cd** (the path moved below the surface), as shown in Fig. 18a and b. The same procedure was followed for specimen 1-I. This specimen with 10.2% moisture content was compressed to 750 kPa (point **a** in Fig. 18a), then unloaded to 430 kPa and the path moved below the VCS (the path of **ae** in Fig. 18a). After wetting, the specimen swelled minorly to hit the surface at **e′** to follow the path of **ee′**. With continuous wetting, the specimen collapsed to follow the path of **e′f** at the surface. Next, the specimen was loaded to 3220 kPa and followed the path from **fg** at the surface as shown in Fig. 18. Finally, the specimen was unloaded to 54 kPa and followed the path of **gh** (the path moved inside the surface).

4. Conclusions

A series of laboratory tests were performed to investigate the suitability of the theory of swelling and collapse proposed based on the virgin compression surface obtained using the modified MPK framework. This study was carried out on unsaturated compacted expansive clay, as well as lime-treated expansive clay stabilized at the OLC.

This study coupled two partial approaches, namely suction and moisture content-based approaches. The mechanism of collapse and swelling based on the VCS (moisture content-based framework) and Alonso et al. (1990) model (suction-based framework) was investigated using the experimental results achieved in this study. The results showed that the collapse and swelling values obtained from both of these frameworks matched well which verified the suitability of the moisture content-based approach (Modified MPK framework).

More importantly, an innovative method to predict the swell or collapse behavior of the samples after wetting was proposed without requiring to establish a virgin compression surface or to measure suction. This method basically requires the identification of the initial condition of the unsaturated specimen including moisture content, void ratio and preconsolidation pressure and the preconsolidation pressure of the saturated specimen.

It was revealed that any specimen collapses if it is prepared at the initial state (moisture content, void ratio and preconsolidation pressure) and wetted under a stress located between the preconsolidation pressure of the unsaturated (at initial state) and saturated specimens. Otherwise, the specimen swells if the specimen is wetted under a stress less than the preconsolidation pressure of the saturated specimen.

It is well known that the loading-collapse for the untreated soil can be represented as a curve; however, a significant finding of this research was that the loading-collapse behavior of lime stabilized soil in σ-s plane can be represented as a relatively straight line. As the modified MPK framework is a moisture content-based theory, σ-w relationship was studied and represented as a curve for both untreated and lime-treated clays. Finally, this research showed the potential of interpreting the experimental results obtained through suction-monitored testing (such as the results reported by Jotisankasa et al. (2007)) into modified MPK framework which is a moisture content-based approach. This offers an approach for conversion of the results between two partial theories.

The industry favors using the conventional parameters including moisture content, void ratio and stress that are commonly used for saturated soils. Since unsaturated suction-based testing requires specialized equipment and expert test engineers, unsaturated geomechanics has not found its way into the practice widely. The outcomes of this research can be used in the geotechnical industry, first to predict the wetting induced collapse/swelling state of the specimen and further, to calculate the amount of collapse using the method proposed as the modified MPK framework by Al-Taie et al. (2019).

References

Abeyrathne, W.J.C.E., 2017. A new modelling approach for compacted clayey soils using specific water volume as a state variable. Doctoral

dissertation. Monash University https://doi.org/10.4225/03/58d888ad55f4a.

Al-Taie, A., Disfani, M., Evans, R., Arulrajah, A., 2019. Collapse and swell of lime stabilized expansive clays in void ratio–moisture ratio–net stress space. Int. J. Geomech. 19 (9), 04019105. https://doi.org/10.1061/(asce)gm.1943-5622.0001488.

Alonso, E.E., Gens, A., Josa, A., 1990. A constitutive model for partially saturated soils. Géotechnique 40 (3), 405–430. https://doi.org/10.1680/geot.1990.40.3.405.

AS1289.3.4.1, 2008. Methods of Testing Soils for Engineering Purposes Soil classification tests - Determination of the linear shrinkage of a soil - Standard method. Sydney, Australia.: Standards Association of Australia https://infostore.saiglobal.com/en-us/standards/as-1289-3-4-1-2008-r2016–128261_saig_as_as_275348.

ASTM-D422, 2007. Standard Test Method for Particle Size Analysis of Soils. West Conshohocken, ASTM International.

ASTM-D698, 2012. Standard Test Methods for Laboratory Compaction Characteristics of Soil Using Standard Effort (12 400 ft-lbf/ft^3 (600 kN-m/m^3)). West Conshohocken, ASTM International https://doi.org/10.1520/d0698-12.

ASTM-D854, 2010. Standard Test Methods for Specific Gravity of Soil Solids by Water Pycnometer. ASTM International, West Conshohocken https://doi.org/10.1520/d0854-10.

ASTM-D2435, 1996. Standard Test Method for One-Dimensional Consolidation Properties of Soils. ASTM International, West Conshohocken https://doi.org/10.1520/d2435-96.

ASTM-D2487, 2011. Standard Practice for Classification of Soils for Engineering Purposes (Unified Soil Classification System). ASTM International, West Conshohocken https://doi.org/10.1520/d2487-11.

ASTM-D4318, 2000. Standard Test Method for Liquid Limit, Plastic Limit, and Plasticity Index of soils. ASTM International, West Conshohocken https://doi.org/10.1520/d4318-00.

ASTM-D5298, 2016. Standard Test Method for Measurement of Soil Potential (Suction) Using Filter paper. ASTM International, West Conshohocken https://doi.org/10.1520/d5298-16.

ASTM-D6836, 2016. Standard Test Methods for Determination of the Soil Water Characteristic Curve for Desorption Using Hanging Column, Pressure Extractor, Chilled Mirror Hygrometer, or Centrifuge. ASTM International, West Conshohocken https://doi.org/10.1520/d6836-16.

Ciancio, D., Beckett, C.T.S., Carraro, J.A.H., 2014. Optimum lime content identification for lime-stabilised rammed earth. Constr. Build. Mater. 53, 59–65. https://doi.org/10.1016/j.conbuildmat.2013.11.077.

Fredlund, D.G., Morgenstern, N.R., 1976. Constitutive relations for volume change in unsaturated soils. Can. Geotech. 13 (3), 261–276. https://doi.org/10.1139/t76-029.

Fredlund, D.G., Rahardjo, H., 1993. Soil Mechanics for Unsaturated Soils. John Wiley & Sons, New York https://books.google.com.au/books?hl=en&lr=&id=Vd7BDwAAQBAJ&oi=fnd&pg=PA1&dq=Fredlund,+D.G.,+Rahardjo,+H.,+1993.+Soil+Mechanics+for+Unsaturated+Soils.+John+Wiley+%26+Sons,+New+York&ots=Ihf5Wf6MYl&sig=WWQySUiBg53eUnG1Hl_fwcxTmqA&redir_esc=y#v=onepage&q=Fredlund%2C%20D.G.%2C%20Rahardjo%2C%20H.%2C%201993.%20Soil%20Mechanics%20for%20Unsaturated%20Soils.%20John%20Wiley%20%26%20Sons%2C%20New%20York&f=false.

Ghasemzadeh, H., Sojoudi, M.H., Ghoreishian Amiri, S.A., Karami, M. H., 2017. Elastoplastic model for hydro-mechanical behavior of unsaturated soils. Soils Found. 57 (3), 371–383. https://doi.org/10.1016/j.sandf.2017.05.005.

Islam, T., 2015. A study of volumetric behaviour of compacted clayey soils in the void ratio, moisture ratio and net stress space. Ph.D. Thesis, Department of Civil Engineering, Monash University, Victoria, Australia https://bridges.monash.edu/articles/thesis/A_study_of_volumetric_behaviour_of_compacted_clayey_soils_in_the_void_ratio_moisture_ratio_and_net_stress_space/4705087.

Islam, T., Kodikara, J., 2016. Interpretation of the loading–wetting behaviour of compacted soils within the "MPK" framework. Part I: Static compaction 1. Can. Geotech. J. 53 (5), 783–805. https://doi.org/10.1139/cgj-2014-0316.

Jotisankasa, Apiniti, Ridley, Andrew, Coop, Matthew, 2007. Collapse behavior of compacted Silty clay in suction-monitored oedometer apparatus. J. Geotech. Geoenviron. Eng. 133 (7), 867–877. https://doi.org/10.1061/(asce)1090-0241(2007)133:7(867).

Kodikara, Jayantha, 2012. New framework for volumetric constitutive behaviour of compacted unsaturated soils. Can. Geotech. J. 49 (11), 1227–1243. https://doi.org/10.1139/t2012-084.

Kodikara, J., Islam, T., Rajeev, P., 2016. Interpretation of the loading–wetting behaviour of compacted soils within the "MPK" framework. Part II: Dynamic compaction 1. Can. Geotech. J. 53 (5), 806–827. https://doi.org/10.1139/cgj-2014-0317.

Kodikara, J., Islam, T., Wijesooriya, S., Bui, H., Burman, B., 2014. On controlling influence of the line of optimums on the compacted clayey soil behaviour. In: Khalili, N., Russell, A.R., Khoshghalb, A. (Eds.), Proceedings of the Sixth International Conference on Unsaturated Soils, UNSAT2014. CRC Press, Sydney, Australia, 219–225 https://doi.org/10.1201/b17034-29.

Loret, Benjamin, Khalili, Nasser, 2002. An effective stress elastic–plastic model for unsaturated porous media. Mech. Mater. 34 (2), 97–116. https://doi.org/10.1016/s0167-6636(01)00092-8.

Lu, Ning, 2008. Is matric suction a stress variable?. J. Geotech. Geoenviron. Eng. 134 (7), 899–905. https://doi.org/10.1061/(asce)1090-0241(2008)134:7(899).

McAndrew, J., Marsden, M.A.H., 1973. Regional Guide to Victorian Geology. School of Geology, University of Melbourne: Parkville, Victoria 3052, Australia http://worldcat.org/isbn/095990610X.

Murray, E.J., Sivakumar, V., 2010. Unsaturated Soils: A Fundamental Interpretation of Soil Behaviour. John Wiley & Sons https://doi.org/10.1201/b10526-10.

Rahardjo, Harianto, Cong Thang, Nguyen, Kim, Yongmin, Leong, Eng-Choon, 2018. Unsaturated elasto-plastic constitutive equations for compacted kaolin under consolidated drained and shearing-infiltration conditions. Soils Found. 58 (3), 534–546. https://doi.org/10.1016/j.sandf.2018.02.019.

Rao, B.H., Venkataramana, K., Singh, D.J.C.G.J., 2011. Studies on the determination of swelling properties of soils from suction measurements 48(3), 375–387 https://doi.org/10.1139/t10-076.

Ridley, A., Burland, J., 1993. A new instrument for the measurement of soil moisture suction. Géotechnique 43 (2), 321–324. https://doi.org/10.1680/geot.1993.43.2.321.

Sheng, Daichao, Fredlund, Delwyn G., Gens, Antonio, 2008. A new modelling approach for unsaturated soils using independent stress variables. Can. Geotech. J. 45 (4), 511–534.

Singh, D.N., Kuriyan, Sneha J., 2003. Estimation of unsaturated hydraulic conductivity using soil suction measurements obtained by an insertion tensiometer. Can. Geotech. J. 40 (2), 476–483. https://doi.org/10.1139/t02-112.

Sivakumar, V., Wheeler, S.J., 2000. Influence of compaction procedure on the mechanical behaviour of an unsaturated compacted clay. Part 1: Wetting and isotropic compression. Géotechnique 50 (4), 359–368. https://doi.org/10.1680/geot.2000.50.4.359.

Takayama, Yusuke, Tachibana, Shinya, Iizuka, Atsushi, Kawai, Katsuyuki, Kobayashi, Ichizo, 2017. Constitutive modeling for compacted bentonite buffer materials as unsaturated and saturated porous media. Soils Found. 57 (1), 80–91. https://doi.org/10.1016/j.sandf.2017.01.006.

Tarantino, Alessandro, Ridley, Andrew M., Toll, David G., 2008. Field measurement of suction, water content, and water permeability. Geotech. Geol. Eng. 26 (6), 751–782. https://doi.org/10.1007/s10706-008-9205-4.

Tripathy, S., Subba Rao, K.S., Fredlund, D.G., 2002. Water content – void ratio swell-shrink paths of compacted expansive soils. Can. Geotech. J. 39 (4), 938–959. https://doi.org/10.1139/t02-022.

UMS, 2013. HYPROP - Laboratory evaporation method for the determination of pF-curves and unsaturated conductivity, 2013.

Available online: http://www.ums-muc.de/en/products/soil_laboratory/hyprop.html (accessed 08-29-2013).

Wheeler, S.J., Sivakumar, V., 1995. An elasto-plastic critical state framework for unsaturated soil. Géotechnique 45 (1), 35–53. https://doi.org/10.1680/geot.1995.45.1.35.

Yaghoubi, Ehsan, Disfani, Mahdi M., Arulrajah, Arul, Kodikara, Jayantha, 2019. Development of a void ratio-moisture ratio-net stress framework for the prediction of the volumetric behavior of unsaturated granular materials. Soils Found. 59 (2), 443–457. https://doi.org/10.1016/j.sandf.2018.12.005.